

Electron Transfer Behavior of Pincer-Type $\{\text{RhNO}\}^8$ Complexes: Spectroscopic Characterization and Reactivity of Paramagnetic $\{\text{RhNO}\}^9$ Complexes

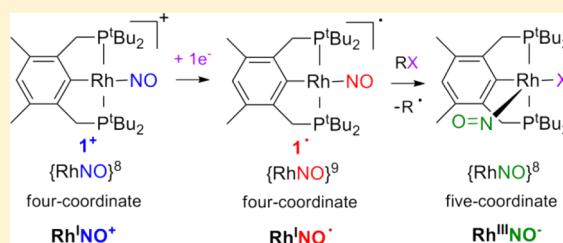
Juan Pellegrino,[†] Carina Gaviglio,[†] David Milstein,[‡] and Fabio Doctorovich^{*†}

[†]Departamento de Química Inorgánica, Analítica, y Química Física, Facultad de Ciencias Exactas y Naturales, Universidad de Buenos Aires, INQUIMAE-CONICET, Ciudad Universitaria, Pab. 2, C1428EHA, Buenos Aires, Argentina

[‡]Department of Organic Chemistry and Department of Chemical Research Support, The Weizmann Institute of Science, Rehovot, 76100, Israel

Supporting Information

ABSTRACT: The electrochemistry of the $\{\text{RhNO}\}^8$ complexes $[\text{Rh}(\text{PCP}^t\text{Bu})(\text{NO})][\text{BF}_4]$ (1^+), $[\text{Rh}(\text{PCP}^t\text{BuCH}_2)(\text{NO})][\text{BF}_4]$ (2^+), and $\text{Rh}(\text{PCP}^t\text{Bu})(\text{NO})\text{Cl}$ (3) was studied. Both four-coordinate complexes 1^+ and 2^+ exhibit a reversible reduction within the CH_2Cl_2 solvent window. Nevertheless, the chemical or electrochemical reduction of 1^+ and 2^+ in CH_2Cl_2 led to the formation of the five-coordinate $\{\text{RhNO}\}^8$ complexes 3 and $\text{Rh}(\text{PCP}^t\text{BuCH}_2)(\text{NO})\text{Cl}$ (4), respectively, through chloride abstraction from CH_2Cl_2 by the one-electron-reduced $\{\text{RhNO}\}^9$ species $[\text{Rh}(\text{PCP}^t\text{Bu})(\text{NO})]^\bullet$ (1^\bullet) and $[\text{Rh}(\text{PCP}^t\text{BuCH}_2)(\text{NO})]^\bullet$ (2^\bullet), as has been observed for many other 17-electron paramagnetic complexes. The new complex 4 was fully characterized by multinuclear NMR techniques, IR, X-ray diffraction, CV, UV–vis, and elemental analysis. On the other hand, the five-coordinate complexes 3 and 4 show only one irreversible oxidation in CH_2Cl_2 and two irreversible reductions in THF. The $\{\text{RhNO}\}^9$ complex 1^\bullet could be obtained quantitatively by one-electron reduction of 1^+ with cobaltocene in nonchlorinated solvents and was characterized by IR, EPR, and ^1H NMR in solution. Activation of carbon–halogen bonds by complex 1^\bullet was observed by studying the reactivity of 1^\bullet with some aryl halides, giving in all cases the $\{\text{RhNO}\}^8$ $\text{Rh}(\text{PCP}^t\text{Bu})(\text{NO})\text{X}$ ($\text{X} = \text{Cl}^-$, 3 , or $\text{X} = \text{I}^-$, 6) as the only rhodium complex, while a complex with coordination of the aryl moiety was not observed as a stable final product in any case. The fate of the aryl organic radicals could be determined in some cases. In addition, DFT calculations were performed to elucidate the electronic structure of 1^\bullet and to support the observed reactivity.



INTRODUCTION

For many years, the chemistry of NO^\bullet has been a topic of great interest to inorganic chemists, and nitrosyl complexes have experienced renewed attention since the discovery of the nitric oxide radical NO^\bullet as a physiologically essential agent.¹ The rich coordination chemistry of the “simple” NO ligand is based on its redox activity, which gives rise to three limiting ($\text{M}^n\text{-NO}^\bullet$, $\text{M}^{n+1}\text{-NO}^-$, and $\text{M}^{n-1}\text{-NO}^+$) and countless intermediate electronic states for metal nitrosyl complexes. In recognition of the covalent nature of the $\text{M}\text{-NO}$ bond, nitrosyl complexes are described as $\{\text{MNO}\}^n$ (regardless of the coligands), where n stands for the number of electrons in the metal d and π^* NO orbitals.^{1d} On the other hand, complexes with pincer ligands constitute an extensive family of compounds that have been steadily attracting increasing interest in view of their important roles in synthesis, bond activation, and catalysis.² It has been demonstrated that the superiority of pincer-complex catalysts over the traditional ones is based on the high stability and well-defined structure and stoichiometry of these species. So it seems interesting to explore the possible “synergistic effect” of the combination of robust bulky pincer ligands (high stability,

well-defined structure, and steric protection) with the non-innocence of the NO ligand (electronic reservoir) in the reactivity of $\{\text{RhNO}\}^n$ complexes.

While there have been many reports on the structure, reactivity, and redox interconversion for five- and six-coordinate $\{\text{MNO}\}^n$ complexes ($n = 6, 7$, and 8),^{1,3} square-planar $\{\text{MNO}\}^8$ complexes are rare. Only a few complexes with iridium were reported many years ago, but their redox behavior was not studied.^{1c,4} In a recent paper,⁵ we reported the synthesis of a family of $\{\text{RhNO}\}^8$ pincer-type complexes (square-planar four-coordinate, formally Rh^{I} , and square-pyramidal five-coordinate, formally Rh^{III} complexes). Also spectroscopic and structural characterization was presented, and their reactivity was studied. Now we wish to focus on the electron transfer behavior of $\{\text{RhNO}\}^8$ complexes to study the electronic structure and the reactivity of $\{\text{RhNO}\}^n$ pincer-type complexes with $n \neq 8$, with special interest in paramagnetic complexes. Since many years ago odd-electron complexes have

Received: August 30, 2013

Published: October 31, 2013

attracted much attention for their use in organic transformations, and there have been several reports on the role of monomeric d^7 17-electron complexes in the activation of carbon–halogen bonds.^{6,7} Also some C–H activation reactions have been observed for Rh(0) complexes.⁸

An interesting approach is the use of redox “noninnocent” ligands as reservoirs of electrons for bond-making and bond-breaking reactions at coordinatively unsaturated metals, with the possibility to store electrons in the ligand, followed by metal-centered reactions. For example, in 2006 Frech et al. reported that the one-electron reduction product of the rhodium(I) pincer naphthyl complex $[(C_{10}H_5(CH_2P^tPr_2)_2)Rh(\eta^1-N_2)]$ shows metal-centered reactivity with water and benzyl chloride, although EPR proved the unpaired electron to be centered at the PCP ligand.⁹ More recently, Zhu et al. showed that the *formally* Co(0) complex $LCo(N_2)$ ($L = 2,6$ -bis(2,6-dimethylphenyliminoethyl)pyridine) with a redox-active iminopyridine ligand reacts with many alkyl and aryl halides RX, including aryl chlorides, to give a mixture of $LCoR$ and $LCoX$ (binuclear oxidative addition) in a halogen atom abstraction mechanism.¹⁰ So, it seems interesting to explore the one-electron reduction products of $\{RhNO\}^8$ complexes, which would be isoelectronic with the *formally* Rh(0) and Co(0) complexes mentioned above and could exhibit similar reactivity.

To our knowledge, very few $\{MNO\}^9$ complexes were previously reported, in contrast with the several $\{MNO\}^n$ systems reported for $n = 4, 5, 6, 7, 8$, and 10, with $n = 9$ being by far the number with fewer examples.¹ Three of these $\{MNO\}^9$ systems are cobalt complexes, and crystal structures were reported,^{11–13} while the other one is a rhodium complex with an anionic PNP pincer ligand, much more related to our system because of the metal and the similar ligand environment.¹⁴ Very recently, Wieghardt and co-workers could provide a qualitative description of the Co–NO bonding in the four-coordinate $\{CoNO\}^9$ species $Tp^*Co(NO)$ ($Tp^* =$ hydrotris(3,5-Me₂-pyrazolyl)borate): through a variety of spectroscopic measurements and DFT calculations, they described it as a Co(II) ($S_{Co} = 3/2$) metal center, antiferromagnetically coupled to a triplet NO[−] anion ($S_{NO} = 1$).¹³ On the other hand, the only $\{RhNO\}^9$ complex reported, $Rh(PNP)NO$ ($PNP = N(tBu_2PCH_2SiMe_2)_2$), could not be isolated but was characterized by IR, NMR, and EPR in solution, and a $Rh^I NO^{\bullet}$ structure was supported by DFT calculations.¹⁴

In this article we report the electron transfer behavior of the four-coordinate $\{RhNO\}^8$ complexes $[Rh(PCP^tBu)(NO)][BF_4]$ (1^+) and $[Rh(PCP^tBuCH_2)(NO)][BF_4]$ (2^+) and the five-coordinate $\{RhNO\}^8$ complex $Rh(PCP^tBu)(NO)Cl$ (3) (Figure 1).

Both complexes 1^+ and 2^+ show accessible reduction potentials, thanks to the presence of the reducible NO moiety, exhibiting a reversible one-electron reduction to a $\{RhNO\}^9$ species. The novel $\{RhNO\}^9$ species 1^{\bullet} was well characterized in solution and its reactivity with organic halides was studied,

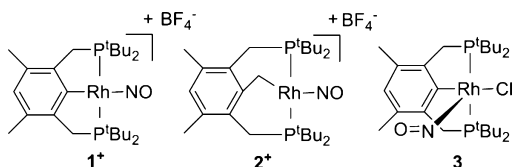


Figure 1. $\{RhNO\}^8$ complexes used in this study.

resulting in C–X bond activation; this reactivity has been not documented for the previously reported $\{RhNO\}^9$ system.

RESULTS AND DISCUSSION

Cyclic Voltammetry. The $\{RhNO\}^8$ complex $[Rh(PCP^tBu)(NO)][BF_4]$ (1^+) exhibits in CH_2Cl_2 one accessible redox process at $E_{1/2} = -1.16$ V within the solvent window (Figure 2a), which can be represented by eq 1.

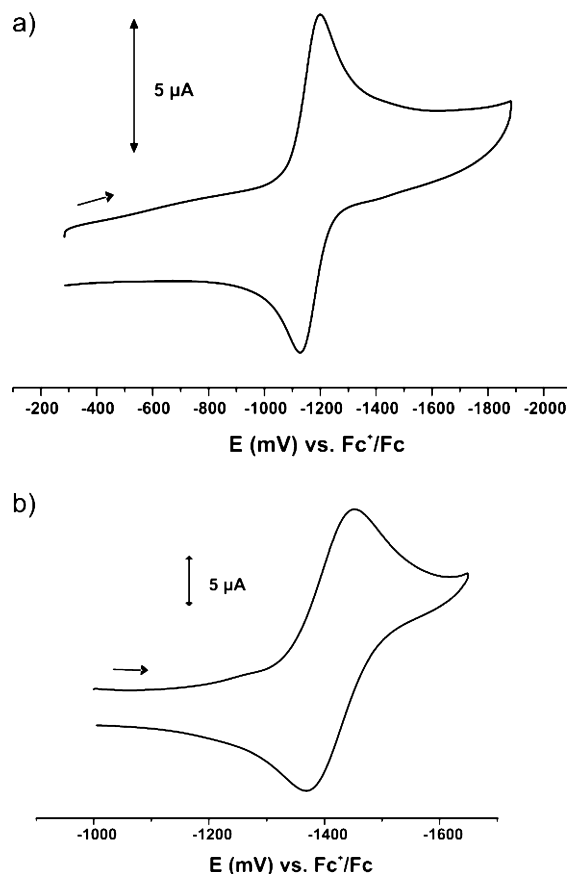
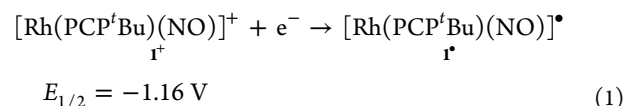
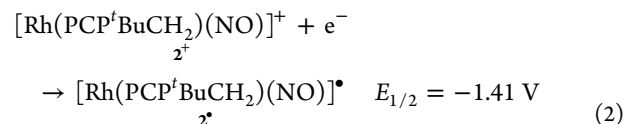


Figure 2. Cyclic voltammograms of 1^+ (a) and 2^+ (b) in $CH_2Cl_2/0.1$ M Bu_4NPF_6 .

The related $\{RhNO\}^8$ complex $[Rh(PCP^tBuCH_2)(NO)][BF_4]$ (2^+) shows a reversible reduction at $E_{1/2} = -1.41$ V (eq 2), which is shifted by -250 mV from the corresponding value of 1^+ (Figure 2b).

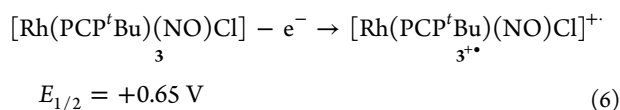
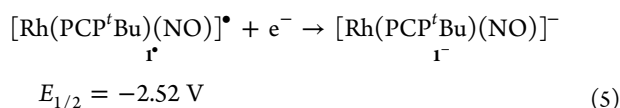
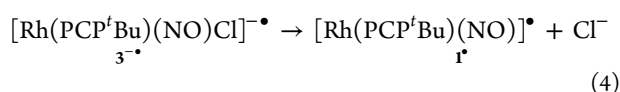
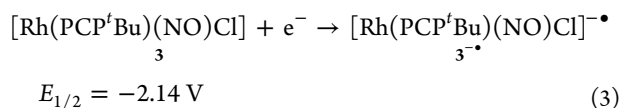


This similar response on electrochemical reduction was expected since both complexes are four-coordinated monocationic nitrosyl Rh(I) complexes, with very similar coligands: phenyl PCP^tBu for 1^+ and benzyl PCP^tBuCH_2 for 2^+ .

The reduction process of complex 2^+ is less favorable than that of 1^+ , consistent with the stronger donation of the benzylic

moiety, as reflected also by its low-energy-shifted NO stretching frequency (1834 vs 1726 cm^{-1} for 1^+ and 2^+ in CH_2Cl_2 , respectively). In contrast with the accessible one-electron reduction of complexes 1^+ and 2^+ , the structurally related Rh(I) complex $\text{Rh}(\text{PCP}^t\text{Bu})(\text{CO})^{15}$ shows no reduction process in the whole broad window of the THF solvent, up to -3.0 V, while complex 1^+ shows a second (irreversible) wave at -2.49 V in that solvent (see CV of 1^+ in THF in the Supporting Information, Figure S1). This proves the ability of the NO ligand to access low oxidation states in these PCP complexes.

In contrast with the reversible reductions observed for the four-coordinate $\{\text{RhNO}\}^8$ complexes 1^+ and 2^+ , the five-coordinate $\{\text{RhNO}\}^8$ complex **3** shows only an irreversible oxidation at 0.65 V in CH_2Cl_2 and two irreversible reductions at -2.14 and -2.52 V in THF (Figure 3, eqs 3–6).



The potential of the last reduction wave is almost identical to that of the second wave of 1^+ in THF (Figure S1), suggesting that the chloride ligand is lost after the first reduction of **3**, giving 1^\bullet , eqs 3–5. The irreversibility of the last reduction (eq 5) could be due to loss of the NO and/or the PCP ligand. In the case of the oxidation, the observation of the reduction wave at -1.16 V of the couple $1^+/1^\bullet$ when scanning the potential in the reverse direction after having reached the oxidation potential of **3** suggested that 1^+ is generated from $3^{+\bullet}$. Also when the chemical or the electrochemical oxidation of **3** was performed, the IR spectra (Figure S2) showed the appearance of the ν_{NO} stretching frequency of 1^+ . These results suggest the loss of chloride radical from $3^{+\bullet}$.

Spectroelectrochemistry and Chemical Reduction of Complexes 1^+ and 2^+ . The reversibility of the reduction wave of complexes 1^+ and 2^+ in CH_2Cl_2 solution inspired us to explore the electrochemical reduction through IR spectroelectrochemistry, since the ν_{NO} stretching band is known to be very sensitive to the oxidation state of this noninnocent ligand in metal complexes.^{1,3}

The IR spectra obtained on electrochemical reduction of 1^+ are presented in Figure 4. The electrolytic reduction of the monocation 1^+ in $\text{CH}_2\text{Cl}_2/0.1$ M Bu_4NPF_6 is accompanied by a 209 cm^{-1} low-energy shift of the NO stretching band from 1834 to 1625 cm^{-1} (Figure 4). Surprisingly, despite the reversibility under CV conditions, reversing the potential did not result in the recovery of the starting material 1^+ . Moreover, the ν_{NO} stretching band observed for the product is the same as that of the known complex $\text{Rh}(\text{PCP}^t\text{Bu})(\text{NO})\text{Cl}$ (**3**), obtained by reaction of 1^+ with chloride.⁵ Consequently, the expected

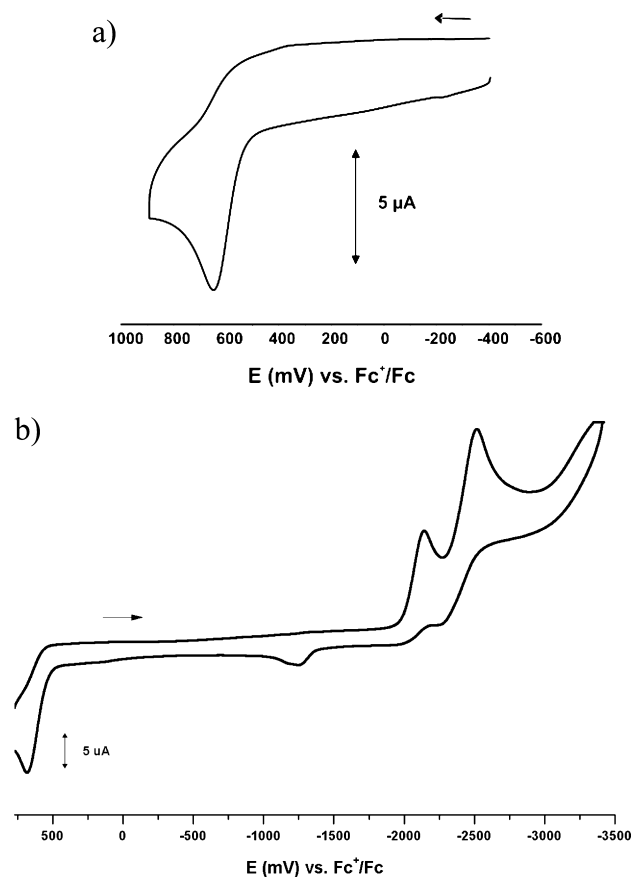


Figure 3. Cyclic voltammogram of **3** in CH_2Cl_2 (a) and THF (b)/0.1 M Bu_4NPF_6 .

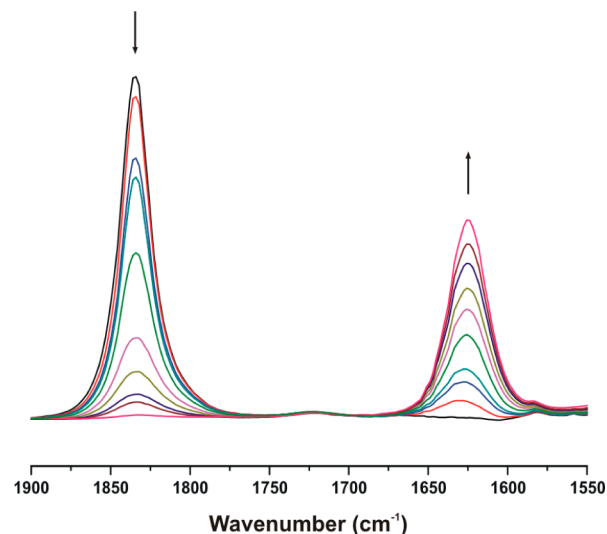
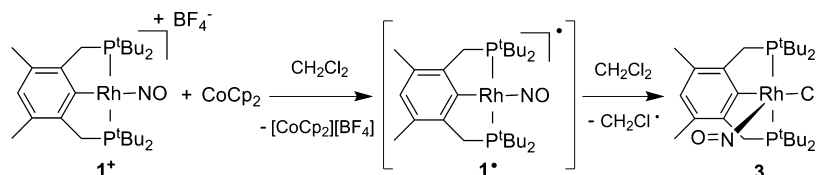


Figure 4. IR spectral changes observed during the electrochemical reduction of 1^+ in $\text{CH}_2\text{Cl}_2/0.1$ M Bu_4NPF_6 .

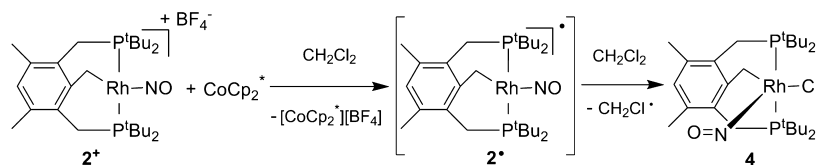
reactive 17-electron species 1^\bullet , although stable on the CV scale, could not be observed under these conditions, and complex **3** is formed, probably by chloride abstraction from CH_2Cl_2 .

In order to confirm the formation of complex **3** by the electrochemical reduction, the chemical reduction of complex 1^+ was tried in CH_2Cl_2 . Considering the reversible reduction wave of 1^+ at $E_{1/2} = -1.16$ V, cobaltocene, $\text{Co}(\text{Cp})_2$ ($\text{Cp} = \text{cyclopentadienyl}$) ($E_{1/2} = -1.33$ V),¹⁶ was chosen as the proper

Scheme 1



Scheme 2



reducing agent. Reaction of 1^+ with 1 equiv of $\text{Co}(\text{Cp})_2$ in CH_2Cl_2 resulted in quantitative formation of 3 and $[\text{Co}(\text{Cp})_2][\text{BF}_4]$, confirming the initial formation of the one-electron-reduced $\{\text{RhNO}\}^9$ species 1^* (Scheme 1). The identity of 3 was confirmed by ^{31}P and ^1H NMR, FTIR, and UV–vis.⁵ The UV–vis spectra for complexes 1^+ , 2^+ , and 3 , not previously reported, are presented in the Supporting Information, Figure S3 and Table S1. So, although the reduced species (1^*) is best described as a Rh(I) with a reduced NO^\bullet ligand (see below), it shows similar reactivity to 17-electron metal-centered radicals,^{6,7} as mentioned in the Introduction. However, one important difference is that in our system the alkyl moiety did not end coordinated to rhodium. The fate of the organic radical ($\text{CH}_2\text{Cl}^\bullet$) was not determined in this experiment, but it could be identified in the reaction between 1^* and some aryl halides (see below).

IR spectroelectrochemistry experiments of complex 2^+ show the same results as complex 1^+ ; the reduced species 2^* is not stable in CH_2Cl_2 . Chemical reduction of 2^+ allowed us to isolate and fully characterize complex $\text{Rh}(\text{PCP}^t\text{BuCH}_2)(\text{NO})\text{Cl}$ (4).

Reaction of 2^+ with CoCp_2^* in CH_2Cl_2 Solution. Formation of 4 . Considering the reduction potential of complex 2^+ , $\text{Co}(\text{Cp}^*)_2$ ($\text{Cp}^* = 1,2,3,4,5$ -pentamethylcyclopentadienyl) ($E_{1/2} = -1.94\text{ V}$)¹⁶ was chosen as the reducing agent. Treatment of complex 2^+ with 1 equiv of $\text{Co}(\text{Cp}^*)_2$ in dichloromethane solution resulted in quantitative formation of 4 as a single new product, also by chloride abstraction from CH_2Cl_2 by the one-electron-reduced $\{\text{RhNO}\}^9$ species 2^* (Scheme 2).

The new complex 4 was fully characterized by multinuclear NMR techniques, IR, X-ray diffraction, CV, UV–vis, and elemental analysis. The $^{31}\text{P}\{^1\text{H}\}$ NMR spectrum of 4 (Figure S4) exhibits a doublet at δ 117.7 with a $^1J_{\text{Rh,P}} = 176.7\text{ Hz}$, indicative of two chemically equivalent phosphorus nuclei coordinated to rhodium (Figure S4). In the ^1H NMR (Figure S5), the methylene group of RhCH_2Ar gives rise to a triplet of doublets positioned at 3.4 ppm ($^2J_{\text{RH}} = 1.9\text{ Hz}$, $^3J_{\text{PH}} = 7.0\text{ Hz}$). The methylene group appears in the $^{13}\text{C}\{^1\text{H}\}$ NMR as a doublet of triplets at 13.4 ppm ($^1J_{\text{RH}} = 16.8\text{ Hz}$, $^2J_{\text{PH}} = 2.6\text{ Hz}$). In the ^{15}N NMR (Figure S6), there is only one signal due to the ^{15}N -enriched nitrosyl complex 4 , which appears at 831.4 ppm as a broad singlet, characteristic of a bound bent nitrosyl.^{17,5} The IR spectrum obtained in the solid state shows a signal characteristic of a nitrosyl ligand at 1605 cm^{-1} (Figure S7), similar to the ν_{NO} stretching frequency of other

square-pyramidal $\{\text{MNO}\}^8$ complexes, as several reported five-coordinate nitrosyl cobalt(III) complexes¹⁷ and the related five-coordinate nitrosyl rhodium(III) complex 3 .⁵ The assignment of the band was confirmed by use of the ^{15}N -labeled derivative $\text{Rh}(\text{PCP}^t\text{BuCH}_2)(^{15}\text{NO})\text{Cl}$, with a frequency at 1572 cm^{-1} . These data are consistent with a bent RhNO moiety.⁵

The molecular structure of 4 was confirmed by an X-ray diffraction study of single crystals obtained by slow diffusion of pentane into a concentrated solution of 4 in CH_2Cl_2 at $-30\text{ }^\circ\text{C}$ (Figure 5). Selective bond lengths and bond angles are given in

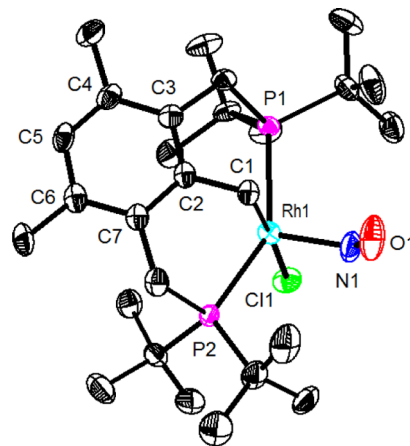


Figure 5. ORTEP plot of complex 4 at the 50% probability level. Hydrogen atoms are omitted for clarity.

Table 1. The rhodium atom is located in the center of a square pyramid with a bent apical nitrosyl group occupying the position *trans* to the empty coordination site and the Cl ligand *trans* to the methylene carbon (C1), with a $\text{C}(1)\text{--Rh}(1)\text{--Cl}(1)$ angle of $176.39(11)^\circ$. Also, it is worth mentioning that the coordinated methylene is tilted out of the plane, with a $\text{Rh}\text{--C}1\text{--C}2$ angle of $101.5(2)^\circ$. As in the case of complex 3 ,⁵ the rhodium atom in complex 4 can be described as Rh(III) with a $\text{Rh}\text{--N}\text{--O}$ angle of $129.6(4)^\circ$, confirming the bent NO character of the nitrosyl ligand, and a $\text{N}\text{--O}$ bond distance of $1.175(6)\text{ \AA}$, both in the range observed for complex 3 ($127.4(3)^\circ$ and $1.184(4)\text{ \AA}$, respectively).⁵

The redox behavior of 4 was studied by cyclic voltammetry; the five-coordinate $\{\text{RhNO}\}^8$ complex 4 exhibits only an irreversible oxidation at 0.65 V in CH_2Cl_2 (Figure S8), at the same potential observed for complex 3 . In order to compare,

Table 1. Selected Bond Lengths (Å) and Angles (deg) for **4**

Rh(1)–C(1)	2.090(4)	C(2)–C(3)	1.416(6)
C(1)–C(2)	1.460(5)	C(3)–C(4)	1.397(6)
Rh(1)–N(1)	1.890(4)	C(4)–C(5)	1.398(6)
N(1)–O(1)	1.175(6)	C(5)–C(6)	1.387(6)
Rh(1)–P(1)	2.4420(10)	C(6)–C(7)	1.403(6)
Rh(1)–P(2)	2.4097(10)	C(7)–C(2)	1.411(6)
		Rh(1)–Cl(1)	2.4615(10)
Rh(1)–N(1)–O(1)	129.6(4)	Rh(1)–C(1)–C(2)	101.5(2)
N(1)–Rh(1)–P(1)	104.75(13)	C(3)–C(2)–C(7)	120.3(4)
N(1)–Rh(1)–P(2)	105.06(12)	C(4)–C(5)–C(6)	123.5(4)
N(1)–Rh(1)–C(1)	89.07(17)	C(2)–C(3)–C(4)	119.2(4)
P(2)–Rh(1)–P(1)	145.18(4)	C(3)–C(4)–C(5)	118.3(4)
N(1)–Rh(1)–Cl(1)	94.54(14)	P(1)–Rh(1)–Cl(1)	97.85(3)
C(1)–Rh(1)–Cl(1)	176.39(11)	P(2)–Rh(1)–Cl(1)	97.31(4)

the electrochemical data for all complexes is summarized in Table 2, along with their ν_{NO} stretching frequencies. The

Table 2. Formal Electrode Potentials and ν_{NO} of the {RhNO}⁸ Complexes in CH₂Cl₂

complex	<i>E</i> (ΔE); volts ^a	ν_{NO} (cm ⁻¹)
1 ⁺	–1.16 (0.072)	1834
2 ⁺	–1.41 (0.083)	1726
3	+0.65	1625
4	+0.65	1615

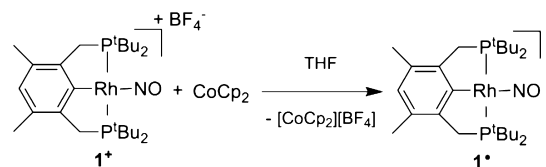
^a*E*_{1/2} (ΔE) for reversible couples and *E*_{pa} for irreversible processes.

striking result is that, while for the four-coordinate {RhNO}⁸ complexes **1**⁺ and **2**⁺ there is an important difference in the electronic structure between the phenyl and benzyl PCP complexes, as concluded by the gap observed in *E* and ν_{NO} , for the five-coordinate {RhNO}⁸ complexes **3** and **4** the difference is negligible. This is consistent with the description of the four-coordinate complexes as Rh^INO⁺, with a dominant back-donation of electron density from the metal center, very influenced by the donor properties of the coligands. On the other hand, the five-coordinate complexes are best described as Rh^{III}NO⁻, for which the back-donation is less important, and accordingly the different donor properties of the phenyl and benzyl ligands are not so relevant to the electronic structure.

Stable {RhNO}⁹ Complex: Preparation and Characterization. We are interested in obtaining the {RhNO}⁹ complex **1**[•] to characterize its electronic structure and explore its reactivity with other organic halides. As stated in the Introduction, {MNO}^{*n*} complexes with *n* = 9 are rare. The only square-planar {RhNO}⁹ complex previously reported, Rh(PNP)NO, was obtained by reaction of a convenient precursor with NO[•], but its reactivity with organic halides was not studied.

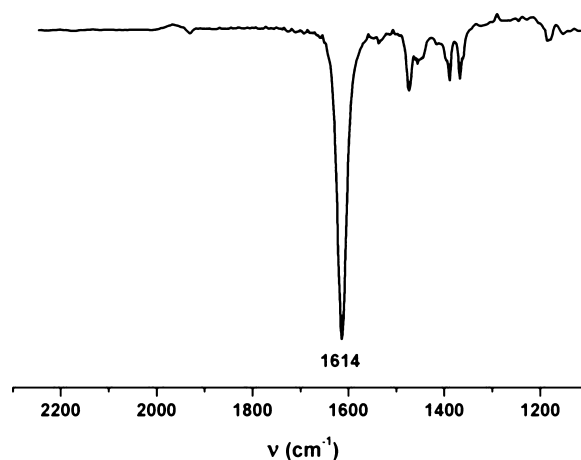
Since the reduction of **1**⁺ in CH₂Cl₂ led to the fast and quantitative formation of **3**, without observing the intermediate {RhNO}⁹ complex **1**[•], we decided to explore the reduction in nonchlorinated solvents. **1**[•] was obtained in nearly quantitative yield when THF or benzene was added to a mixture of **1**⁺ and Co(Cp)₂, both in solid form, under argon (Scheme 3), obtaining a very intense brown solution and a yellow precipitate of [Co(Cp)₂]⁺[BF₄]⁻ within a few minutes.

The paramagnetic nature of **1**[•] was immediately apparent from the ¹H NMR of the supernatant, with broad resonances occurring at δ 24.3 (s, 4H), 3.0 (s, 36H), –11.1 (s, 6H), and

Scheme 3

–37.2 (s, 1H) (Figure S9). The signals are quite broad, and the partitions due to the ¹H coupling with the nuclei ³¹P and ¹⁰³Rh, usually found in related diamagnetic complexes, are not observed. Also consistent with ¹H NMR, the ³¹P{¹H} NMR shows only very weak signals attributed to diamagnetic byproducts, one of those identified as the known Rh(PCP^tBu)–(N₂) (**5**).¹⁸

The IR spectrum of **1**[•] in THF solution (Figure 6) exhibits a very strong band at 1614 cm⁻¹, assigned, on the basis of its

**Figure 6.** IR spectrum of **1**[•] in THF.

relative intensity and position, to the N–O stretching of **1**[•], while the strong ν_{N_2} of **5** at 2123 cm⁻¹ is not observed, confirming it is a minor byproduct.

The EPR spectrum of **1**[•] in THF solution (Figure S10) shows a signal at $g_{\text{iso}} = 2.0011$, but the partition due to coupling with the ¹⁴N or ¹⁵N nucleus was not observed. The related {RhNO}⁹ complex, Rh(PNP)NO, showed a triplet at $g_{\text{iso}} = 2.0064$ with a hyperfine coupling constant $A_{\text{iso}} = 13$ G.¹⁴ The absence of partition could indicate a lower localization of the spin on NO for **1**[•], which is also consistent with the highly shifted signals in the ¹H NMR spectrum, in the range +24 to –37 ppm.

However, the large change of 220 cm⁻¹ in the ν_{NO} observed upon the {RhNO}^{8→9} conversion from **1**⁺ to **1**[•] (1834 to 1614 cm⁻¹) suggests a highly NO-centered reduction, converting a {RhNO}⁸ complex described mainly as Rh^INO⁺ to a {RhNO}⁹ species with a predominant Rh^INO[•] character, in marked contrast with the Co^{II}NO⁻ formulation found for Tp^{*}Co(NO).¹³ This distinct description for **1**[•] as compared to Tp^{*}Co(NO) was expected, given the different series of the transition metal center and the very different nature of the tridentate ligands Tp^{*} and PCP.

The predominant participation of the NO orbitals in the {RhNO}^{8→9} conversion from **1**⁺ to **1**[•] is similar to what has been found in the {MNO}^{6→7} one-electron conversion for many different systems (five- or six-coordinate), with M = Fe^{II},

Ru^{II}, Os^{II}, and Ir^{III}.^{1b,3} This suggests that the NO ligand in five- or six-coordinate {MNO}⁶ and in the square-planar four-coordinate {RhNO}⁸ complexes (such as **1**⁺) has similar electron density, and both systems are best described as NO⁺ complexes, reflected in the high stretching ν_{NO} frequencies in the range 1800–1950 cm⁻¹ and the linear M–N–O angle found for these systems.^{1,3,5} The relatively low ν_{NO} of **1**⁺ and the rather low Rh–N–O angle of 159.9° are due to strong sigma-donation by the aryl ring, as discussed previously.^{5,19} On the other hand, the unpaired electron in both reduced species {MNO}⁷ and {RhNO}⁹ is partially located on the NO ligand, yielding NO[•] complexes, with ν_{NO} in the range 1600–1700 cm⁻¹ and M–N–O angles between 140° and 150°.^{1,3} (see the DFT-optimized structure for the {RhNO}⁹ complex **1**[•] below). However, there are no reports on {MNO}⁷ complexes describing halogen–carbon activation reactivity, in contrast to what we have found for the {RhNO}⁹ species **1**[•].

Reactivity of **1[•] toward RX Compounds.** With the aim to explore the activation of carbon–halogen bonds, the reaction of **1**[•] with some aryl halides was studied. The reactions of **1**[•] with iodobenzene, 2-iodofluorobenzene, CH₂Cl₂, and 4-chloro- α,α,α -trifluorotoluene, were performed in benzene or toluene.

When the reaction of **1**[•] with iodobenzene was performed in toluene, almost quantitative conversion to Rh(PCP^tBu)(NO)I (**6**) was observed after some minutes, as judged by ³¹P{¹H} NMR. In the case of the reaction of **1**[•] with 2-iodofluorobenzene in benzene, quantitative conversion to **6** was observed within minutes, while the product 2-fluorobiphenyl was detected by ¹⁹F NMR (Figure S12) and GC-MS. The identity of **6** was also confirmed by its independent preparation from **1**⁺ and KI (see the Supporting Information).

In the case of the reaction of **1**[•] with CH₂Cl₂ in toluene, also quantitative conversion to **3** was observed within hours, as judged by ³¹P{¹H} NMR.

When the reaction of **1**[•] with 4-chloro- α,α,α -trifluorotoluene was performed in benzene, quantitative conversion of **1**[•] to **3** was observed within hours (Figure S11), but no new signal appeared in the ¹⁹F NMR, probably due to a similar shift of the substrate 4-chloro- α,α,α -trifluorotoluene and the possible products such as 4-trifluoromethylbiphenyl. Fortunately the product 4-trifluoromethylbiphenyl could be identified by GC-MS.

The conversion of **1**[•] to {RhNO}⁸ Rh(PCP^tBu)(NO)X (X = Cl⁻, **3**, or X = I⁻, **6**) as the only rhodium complex was observed in all cases, while a complex with coordination of the aryl moiety was not observed as a stable final product in any case.

DFT Calculations. Density functional theory calculations were performed to obtain more insight into the electronic structure of the {RhNO}⁹ **1**[•] and to support the proposed reactivity of **1**[•] and **2**[•] with organic halides.

Figure 7 shows the HOMO and LUMO of **1**⁺ and the SOMO of **1**[•]. As can be seen, the LUMO of **1**⁺ and the SOMO of **1**[•]

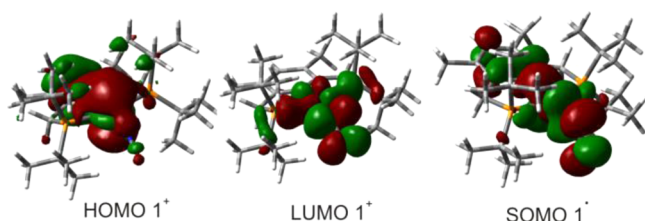


Figure 7. Frontier orbitals of **1**⁺ and **1**[•].

of **1**[•] have a very important contribution of the π^* NO orbital, which suggests a highly NO-centered reduction. Consistent with this, DFT calculations predict a 148 cm⁻¹ decrease of ν_{NO} for the reduction of **1**⁺ to **1**[•] (from 1816 to 1668 cm⁻¹), a rather lower shift than the 220 cm⁻¹ decrease observed in the experiment. However, DFT functionals usually tend to overestimate the electronic density delocalization, thus predicting a smaller $\Delta\nu_{\text{NO}}$ for the electron transfer process, as have been already observed previously for calculations in other nitrosyl complexes.²⁰ So, the IR results along with the DFT calculations support a predominant Rh^INO[•] description for **1**[•], also in agreement with the calculated spin densities of 0.16 on Rh, 0.47 on N, and 0.27 on O.

The optimized structure of **1**[•] is shown in Figure 8, while relevant bond distances and angles, compared to those of **1**⁺,

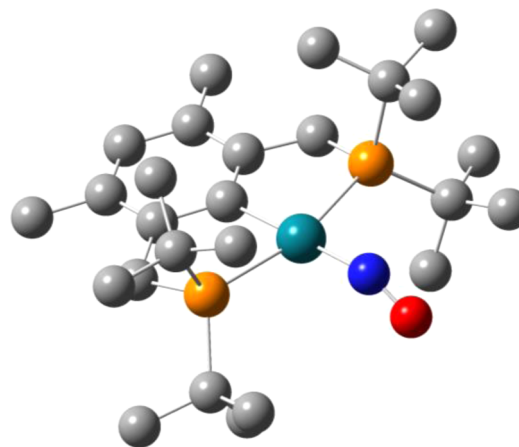


Figure 8. DFT-optimized structure of **1**[•] (hydrogen atoms are omitted for clarity).

Table 3. Selected Bond Lengths (Å) and Angles (deg) for Calculated Structures of **1**⁺ and **1**[•]

	1 ⁺ ^a	1 [•]
<i>d</i> (Rh–C _{ipso})	2.072 (2.085)	2.102
<i>d</i> (Rh–N)	1.812 (1.763)	1.902
<i>d</i> (N–O)	1.175 (1.175)	1.205
\angle Rh–N–O	154.5 (159.9)	148.8

^aExperimental values in parentheses.⁵

are given in Table 3. The lengthening of the Rh–N and N–O distances and the decreasing of the Rh–N–O angle upon the {RhNO}^{8→9} conversion from **1**⁺ to **1**[•] (Table 3) are reminiscent of what is typically observed for the {MNO}^{6→7} conversion of previously reported systems, reflecting a high degree of NO reduction.^{1,3}

It has been proposed previously that the initial step for the reaction of a 17-electron paramagnetic complex with organic halides is halogen abstraction,^{6a,b,7,10} and we propose the same for **1**[•] and **2**[•]. As a difference from previously reported systems, the reactions of **1**[•] and **2**[•] with CH₂Cl₂ give exclusively the five-coordinate complexes with Cl⁻ as a fifth ligand, and the complex with the alkyl fragment, i.e., CH₂Cl⁻, is not observed. The following sequence of reactions is proposed to explain the observed reactivity for **1**[•] and **2**[•], represented as Rh(L)(NO)[•]

(L as a generic representation of PCP^tBu and PCP^tBuCH₂), supported by DFT calculations (Table 4).

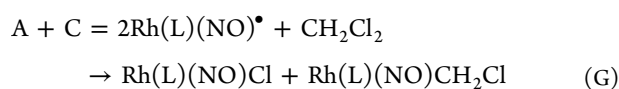
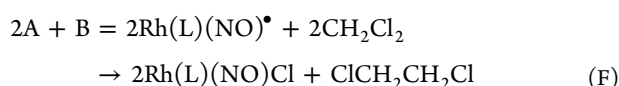
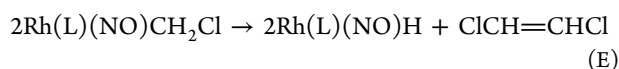
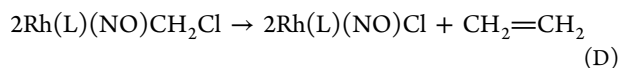
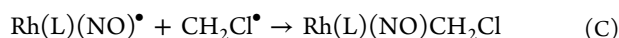
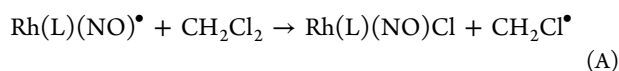
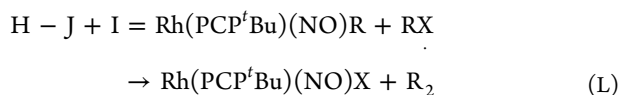
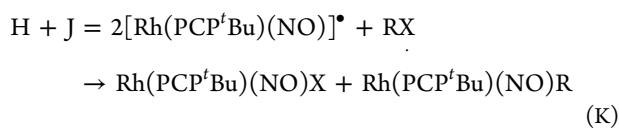
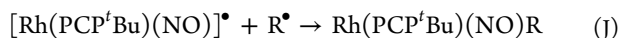
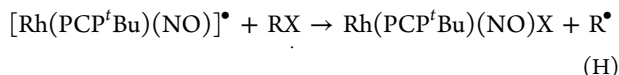


Table 4. Calculated Energies (kcal/mol) for Reactions A and D–G

	1 [•]	2 [•]
A	+4	+9
F	−83	−37
G	−32	−23
D	−67	−69
E	+16	−4

As can be seen, the DFT calculations predict a favorable chloride abstraction from dichloromethane for both 1[•] and 2[•] (entries 1, 2, and 3 in Table 4). The low stability of the five-coordinate alkyl complex (not observed) is also well reproduced, since if it is transiently formed, it will decompose, giving the five-coordinated chloride complexes (the only products observed) (entries 4 and 5 in Table 4). The calculated energies for reactions D and E are also consistent with the absence of a five-coordinated hydride complex (not observed) as a final stable product.

DFT calculations also predict favorable reactions of 1[•] with aryl halides as concluded by the calculated energies for reactions H, K, and L for different aryl halides (Table 5).



As can be observed, DFT calculations predict that reaction L is favorable in all cases, supporting the instability of the five-coordinate aryl complexes Rh(PCP^tBu)(NO)R, in agreement

Table 5. Calculated Energies (kcal/mol) for the Reactions of 1[•] with Aryl Halides

RX	H	K	L
chlorobenzene	+20	−25	−53
bromobenzene	+6	−39	−67
iodobenzene	+6	−39	−67
2-iodofluorobenzene	+6	−46	−63
4-chloro- α,α,α -trifluorotoluene	+20	−27	−53

with the quantitative conversion of 1[•] to the five-coordinate Rh(PCP^tBu)(NO)X, with X = Cl or I, observed in the reaction of 1[•] with aryl halides.

As the expected coupling products dichloroethane (ClCH₂CH₂Cl) and (Aryl)₂ were not detected in the reactions of 1[•] with CH₂Cl₂ and aryl halides, respectively, we can conclude that the thermodynamically feasible reactions B and I do not compete favorably with other faster reactions of the initially generated alkyl and aryl radicals. One of such reactions could involve the solvent, giving the 4-trifluoromethylbiphenyl and 2-fluorobiphenyl products, observed in the reactions of 1[•] with 4-chloro- α,α,α -trifluorotoluene and 2-iodofluorobenzene in benzene, respectively. The attack of an aryl radical to benzene has been already proposed in the literature.²¹ Also, it is possible that the five-coordinate complexes Rh(L)(NO)CH₂Cl and Rh(PCP^tBu)(NO)Aryl are never formed due to the fast reaction of the CH₂Cl[•] and Aryl[•] radicals with the solvent.

CONCLUSIONS

The electron transfer behavior of pincer-type {RhNO}⁸ complexes was studied. The five-coordinate complex 3 shows only irreversible processes due to loss of chloride, while the four-coordinate complexes 1⁺ and 2⁺ exhibit reversible one-electron reductions in CH₂Cl₂. While these {RhNO}^{8–9} conversions are reversible under the cyclic voltammetry conditions, the electrochemical or chemical reduction of 1⁺ and 2⁺ in CH₂Cl₂ did not yield the paramagnetic {RhNO}⁹ complexes 1[•] and 2[•], but the diamagnetic five-coordinate {RhNO}⁸ complexes 3 and 4, by reaction with CH₂Cl₂. The halogen–carbon bond activation reactivity of complex 1[•] was not limited only to its reaction with CH₂Cl₂. Complex 1[•], obtained by reduction of 1⁺ with cobaltocene in nonchlorinated solvents, also reacted with other organic halides, including aryl chlorides, added in slight excess (no more than 5 equivalents). In the absence of halogenated substrates, 1[•] is stable enough to be well characterized in solution. The −220 cm^{−1} shift observed for the ν_{NO} upon the {RhNO}^{8–9} conversion is indicative of a highly NO-centered reduction, similar to what was previously observed for the {MNO}^{6–7} conversion for many five- or six-coordinate complexes. This, along with the DFT calculations, supports a predominant Rh¹NO[•] description for 1[•]. The odd electron in 1[•] is highly located on the NO ligand, as has been found for many five- or six-coordinate {MNO}⁷ complexes, which show ν_{NO} in the range 1600–1700 cm^{−1}, matching well with the value of 1614 cm^{−1} found for 1[•]. However, the metal-centered reactivity found for 1[•], i.e., its reaction with organic halides, has not been documented for the {MNO}⁷ systems or for the few {MNO}⁹ systems previously reported. Studies on the redox behavior of four-coordinate {RhNO}⁸ complexes with other pincer ligands with different electronic and steric properties are under way.

EXPERIMENTAL SECTION

1. Syntheses. All experiments with metal complexes and phosphine ligands were carried out under an atmosphere of purified nitrogen in an MBraun glovebox or using standard Schlenk techniques under an argon atmosphere. All solvents were analytical grade or better. CH_2Cl_2 was distilled over calcium hydride under nitrogen. All other nondeuterated solvents were refluxed over sodium/benzophenone ketyl and distilled under nitrogen. Deuterated solvents were dried over 3 Å molecular sieves. Commercially available reagents were used as received, except for CoCp_2 and CoCp_2^* , which were purified by sublimation. 4-Chloro- α,α,α -trifluorotoluene, iodobenzene, and 2-iodofluorobenzene were stored over 3 Å molecular sieves. $[\text{Rh}(\text{PCP}^t\text{Bu})(\text{NO})][\text{BF}_4]$, $[\text{Rh}(\text{PCP}^t\text{BuCH}_2)(\text{NO})][\text{BF}_4]$, and $\text{Rh}(\text{PCP}^t\text{Bu})(\text{NO})(\text{Cl})$ were prepared as described in a previous work,⁵ with some minor modifications as follows: $[\text{Rh}(\text{PCP}^t\text{Bu})(\text{NO})][\text{BF}_4]$ was prepared in toluene instead of dioxane, and $[\text{Rh}(\text{PCP}^t\text{BuCH}_2)(\text{NO})][\text{BF}_4]$ was further purified by repeated recrystallizations from CH_2Cl_2 -dioxane.

2. Physical Measurements. Cyclic voltammetry was carried out at a 100 mV/s scan rate in dry and deoxygenated $\text{CH}_2\text{Cl}_2/0.1$ M Bu_4NPF_6 using a three-electrode configuration (glassy carbon or Pt working electrode, Pt counter electrode, Pt wire pseudoreference electrode) and a TEQ 03 potentiostat. The ferrocenium/ferrocene ($\text{Fc}^{+/0}$) couple served as an internal reference. All the potentials are expressed against $\text{Fc}^{+/0}$. The solutions were prepared under an atmosphere of purified nitrogen or argon as described before at concentrations of approximately 1 mM. UV-vis spectra were acquired on a Hewlett-Packard HP8453 diode array spectrometer with 1 cm path length cells, under Ar or N_2 , preparing the solutions in a drybox or using standard Schlenk techniques. IR spectra were obtained using a Nicolet Avatar FTIR spectrophotometer. Spectroelectrochemistry was performed by use of an OTTE cell, in dry and deoxygenated $\text{CH}_2\text{Cl}_2/0.1$ M Bu_4NPF_6 . ^1H , ^{13}C , ^{15}N , ^{19}F , and ^{31}P NMR spectra were recorded using a Bruker 500 MHz NMR spectrometer. ^1H and $^{13}\text{C}\{^1\text{H}\}$ NMR chemical shifts are reported in ppm downfield from tetramethylsilane. ^1H NMR chemical shifts were referenced to the residual hydrogen signal of the deuterated solvent (7.15 ppm, benzene; 5.32 ppm, dichloromethane). In $^{13}\text{C}\{^1\text{H}\}$ NMR measurements the signals of deuterated benzene (128.0 ppm) or deuterated dichloromethane (53.8 ppm) were used as a reference. ^{31}P NMR chemical shifts were reported in ppm downfield from H_3PO_4 and referenced to an external 85% solution of phosphoric acid in D_2O . ^{15}N NMR chemical shifts were reported in ppm relative to liquid ammonia. Abbreviations used in the description of NMR data are as follows: br, broad; s, singlet; d, doublet; t, triplet; q, quartet; m, multiplet; v, virtual. EPR measurements were recorded on a Bruker EMX Plus spectrometer. Elemental analysis was performed in a Carlo Erba EA 1108. GC-MS was measured in a Shimadzu, QP-5000.

3. Computational Methodology. All calculations were carried out with the program package Gaussian03.²² The structures of all molecules were fully geometry optimized at the DFT level, using the PBE exchange-correlation functional. The LANL2DZ basis set and pseudopotential were used for the rhodium atom. For the H, N, O, C, P, and F atoms the 6-31G** basis set was used, while for Br and I atoms the LANL2DZ basis set and pseudopotential were used. The vibrational frequencies were calculated on optimized structures using the same functional and basis set.

Reaction of $[\text{Rh}(\text{PCP}^t\text{Bu})(\text{NO})][\text{BF}_4]$ (1^+) with CoCp_2 in CH_2Cl_2 Solution. Formation of $\text{Rh}(\text{PCP}^t\text{Bu})(\text{NO})\text{Cl}$ (3**).** Dichloromethane was added to a mixture of solid 1^+ (8 mg, 0.012 mmol) and solid CoCp_2 (2.4 mg, 0.012 mmol). Immediately a brown solution and a yellow precipitate were obtained. After filtration and evaporation of the solvent the known complex **3** was obtained in nearly quantitative yield. $^{31}\text{P}\{^1\text{H}\}$ and ^1H NMR and IR were the same as reported before.⁵

Reaction of $[\text{Rh}(\text{PCP}^t\text{BuCH}_2)(\text{NO})][\text{BF}_4]$ (2^+) with CoCp_2^* in CH_2Cl_2 Solution. Formation of $\text{Rh}(\text{PCP}^t\text{Bu})(\text{CH}_2)(\text{NO})\text{Cl}$ (4**).** Dichloromethane was added to a mixture of solid 2^+ (15 mg, 0.023 mmol) and solid CoCp_2^* (7.5 mg, 0.023 mmol). Immediately a reddish-brown solution was obtained. $^{31}\text{P}\{^1\text{H}\}$ NMR revealed quantitative formation

of **4** as a single product. After solvent evaporation it was redissolved in toluene. After filtration and evaporation of the solvent the new complex **4** was obtained in nearly quantitative yield. Single crystals suitable for X-ray diffraction were obtained by crystallization from a concentrated solution of **4** in dichloromethane at -30 °C.

Characterization of **4.** $^{31}\text{P}\{^1\text{H}\}$ NMR (CD_2Cl_2): 117.70 (d, $^1J_{\text{RHP}} = 176.7$ Hz). ^1H NMR (CD_2Cl_2): 6.53 (s, 1H, Rh-Ar), 3.42 (vdt, $^3J_{\text{PH}} = 7.0$ Hz, $^2J_{\text{RHH}} = 1.9$ Hz, 2H, Ar- CH_2 -Rh), 3.35 (dq, left part of ABq, $^2J_{\text{HH}} = 14.7$ Hz, 2H, Ar- CH_2 -P), 3.11 (br d, right part of ABq, $^2J_{\text{HH}} = 14.8$ Hz, 2H, Ar- CH_2 -P), 2.27 (s, 6H, 2 Ar- CH_3), 1.26 (vt, $^3J_{\text{PH}} = 5.9$ Hz, 18H, 2 (CH_3)₃C-P), 1.23 (br s, 18H, 2 (CH_3)₃C-P). $^{13}\text{C}\{^1\text{H}\}$ NMR (CD_2Cl_2): 143.67 (br s, Rh-Ar), 132.22 (vt, $^3J_{\text{PC}} = 2.1$ Hz, Rh-Ar), 131.52 (s, Rh-Ar), 126.90 (s, Rh-Ar), 38.87 (br s, (CH_3)₃C-P), 38.26 (vt, $^1J_{\text{PC}} = 2.8$ Hz, (CH_3)₃C-P), 30.94 (vt, $^2J_{\text{PC}} = 1.7$ Hz, (CH_3)₃C-P), 29.40 (vt, $^2J_{\text{PC}} = 1.8$ Hz, (CH_3)₃C-P), 20.20 (vt, $^1J_{\text{PC}} = 6.2$ Hz, Ar- CH_2 -P), 19.83 (s, CH_3 -Ar), 13.39 (br dt, $^1J_{\text{RHC}} = 16.8$ Hz, $^2J_{\text{PC}} = 2.6$ Hz, Ar- CH_2 -Rh) (assignment of $^{13}\text{C}\{^1\text{H}\}$ NMR signals was confirmed by ^{13}C DEPT135). IR ν (solid state, cm^{-1}): 1605 (s, NO). Anal. Calcd: C, 53.69; H, 8.18. Found: C, 53.77; H, 8.24.

X-ray Structural Analysis of **4.** Crystal Data: $\text{C}_{27}\text{H}_{49}\text{ClINOP}_2\text{Rh}$, red, plate, $0.60 \times 0.40 \times 0.30$ mm³, monoclinic; P 1 21/n 1; $a = 10.4103(4)$ Å, $b = 23.0450(7)$ Å, $c = 12.0078(4)$ Å; $\beta = 94.001(3)^\circ$, from 25 degrees of data; $T = 150(2)$ K; $V = 2873.71(17)$ Å³, $Z = 4$; $fw = 603.97$; $D_c = 1.396$ g/cm³; $\mu = 0.819$ mm⁻¹. Data Collection and Processing: Oxford Gemini E CCD area detector diffractometer, Mo $K\alpha$ ($\lambda = 0.71073$ Å), graphite monochromator; $-14 \leq h \leq 10$, $-27 \leq k \leq 30$, $-16 \leq l \leq 15$, 23 053 reflections collected, 6736 independent reflections ($R_{\text{int}} = 0.0281$). For data collection, cell refinement, and data reduction CrysAlisPro software was used. Absorption correction was made by multiscan. Solution and Refinement: The structure was solved by direct methods with SHELXS-97. Full-matrix least-squares refinement based on F^2 with SHELXL-97; 302 parameters with 0 restraints, final $R_1 = 0.0531$ (based on F^2) for data with $I > 2\sigma(I)$, and $R_1 = 0.0620$ on 6736 reflections, goodness-of-fit on $F^2 = 1.044$, largest electron density peak = 4.231 e Å⁻³.

Reaction of $[\text{Rh}(\text{PCP}^t\text{BuCH}_2)(^{15}\text{NO})][\text{BF}_4]$ (2^+) with CoCp_2^* in CH_2Cl_2 Solution. Formation of $\text{Rh}(\text{PCP}^t\text{Bu})(\text{CH}_2)(^{15}\text{NO})\text{Cl}$ (4**).** It was prepared as described above, using $^{15}\text{NOBF}_4$.²³

Characterization of ^{15}N -Labeled **4.** ^{15}N NMR (CD_2Cl_2): 831.38 (br s). IR ν (solid state; cm^{-1}): 1572 (s, ^{15}NO).

Reaction of $[\text{Rh}(\text{PCP}^t\text{Bu})(\text{NO})][\text{BF}_4]$ (1^+) with CoCp_2 in Nonchlorinated Solvents. Formation of $[\text{Rh}(\text{PCP}^t\text{Bu})(\text{NO})]^*$ (1^*). THF or benzene (0.85 mL), deaerated through several freeze-pump-thaw cycles and argon refilling, was added to a mixture of 1^+ (12 mg, 0.019 mmol) and CoCp_2 (3.6 mg, 0.019 mmol) under argon. Immediately a strong brown solution and a light brown precipitate were obtained. The precipitate (identified as $[\text{CoCp}_2][\text{BF}_4]$ by ^1H and ^{19}F NMR) was separated by filtration. $^{31}\text{P}\{^1\text{H}\}$, ^1H NMR, IR, and EPR of the solution indicate nearly quantitative formation of 1^* .

Characterization of 1^* . ^1H NMR (THF): 24.32 (br s, 4H, 2 Ar- CH_2 -P), 3.00 (br s, 36H, 4 (CH_3)₃C-P), -11.12 (br s, 6H, 2 Ar- CH_3), -37.22 (br s, 1H, Rh-Ar). IR ν (in THF solution, cm^{-1}): 1614 (s, NO).

Reaction of $[\text{Rh}(\text{PCP}^t\text{Bu})(\text{NO})]^*$ (1^*) with RX Halides in Benzene or Toluene. Formation of $\text{Rh}(\text{PCP}^t\text{Bu})\text{X}(\text{NO})$. Complex 1^* was prepared as previously described, and then the RX halide was added. The reaction was followed in time by ^1H , ^{19}F , and ^{31}P NMR. Also GC-MS was used to identify the possible organic products.

Reaction of $[\text{Rh}(\text{PCP}^t\text{Bu})(\text{NO})][\text{BF}_4]$ (1^+) with KI. Formation of $\text{Rh}(\text{PCP}^t\text{Bu})(\text{NO})\text{I}$ (6**).** CH_2Cl_2 (1 mL) and CH_3OH (0.5 mL) were added to a mixture of 1^+ (8.5 mg, 0.013 mmol) and KI (3.5 mg, 0.021 mmol). A brown solution was obtained after some minutes' stirring, and through FTIR quantitative formation of **6** was observed. The solvent was removed under vacuum, and the remaining solid was extracted with benzene. The new compound **6** was quantitatively obtained after solvent evaporation.

Characterization of **6.** $^{31}\text{P}\{^1\text{H}\}$ NMR (C_6D_6): 75.40 (d, $^1J_{\text{RHP}} = 143.7$ Hz). ^1H NMR (C_6D_6): 6.66 (s, 1H, Rh-Ar), 3.14 (AB quartet, $^2J_{\text{HH}} = 14.5$ Hz, 4H, Ar- CH_2 -P), 2.19 (s, 6H, 2 Ar- CH_3), 1.21 (vt, $J_{\text{PH}} = 8.3$ Hz, 18H, 2 (CH_3)₃C-P), 1.19 (vt, $J_{\text{PH}} = 7.7$ Hz, 18H, 2 (CH_3)₃C-

P). $^{13}\text{C}\{^1\text{H}\}$ NMR (C_6D_6): 169.98 (d, $^2J_{\text{RhC}} = 40.2$ Hz, C_{ipso} , Rh-Ar), 145.07 (vt, $J_{\text{PC}} = 7.9$ Hz, Rh-Ar), 130.81 (vt, $J_{\text{PC}} = 8.4$ Hz, Rh-Ar), 128.58 (s, C_{para} , Rh-Ar), 37.34 (vt, $J_{\text{PC}} = 6.9$ Hz, $(\text{CH}_3)_3\text{C-P}$), 36.34 (vt, $J_{\text{PC}} = 7.3$ Hz, $(\text{CH}_3)_3\text{C-P}$), 31.70 (vtd, $J_{\text{PC}} = 10.5$ Hz, $^2J_{\text{RhC}} = 2.0$ Hz, Ar- $\text{CH}_2\text{-P}$), 30.80 (vt, $J_{\text{PC}} = 2.2$ Hz, $(\text{CH}_3)_3\text{C-P}$), 28.86 (vt, $J_{\text{PC}} = 2.3$ Hz, $(\text{CH}_3)_3\text{C-P}$), 22.51 (s, $\text{CH}_3\text{-Ar}$) (assignment of $^{13}\text{C}\{^1\text{H}\}$ NMR signals was confirmed by ^{13}C DEPT135). IR ν (solid state; cm^{-1}): 1616 (s, NO). Anal. Calcd: C, 47.65; H, 7.23. Found: C, 47.42; H, 7.21.

■ ASSOCIATED CONTENT

■ Supporting Information

CIF file containing X-ray crystallographic data for **4**. Figures of cyclic voltammogram of $\mathbf{1}^+$; IR spectroelectrochemical oxidation of **3** to $\mathbf{3}^+$; UV-vis spectral data for $\mathbf{1}^+$, $\mathbf{2}^+$, **3**, and **4**; $^{31}\text{P}\{^1\text{H}\}$, ^1H , and ^{15}N spectra of **4**; IR spectra of **4** and ^{15}N -labeled **4**; cyclic voltammogram of **4**; ^1H spectrum of $\mathbf{1}^+$; X-band EPR of $\mathbf{1}^+$; ^{31}P NMR monitoring of the reaction of $\mathbf{1}^+$ with 4-chloro- α,α,α -trifluorotoluene; ^{19}F NMR of the reaction of $\mathbf{1}^+$ with 2-iodofluorobenzene; $^{31}\text{P}\{^1\text{H}\}$, ^1H , and $^{13}\text{C}\{^1\text{H}\}$ spectra of **6**; Cartesian coordinates from optimizations for all rhodium complexes. This material is available free of charge via the Internet at <http://pubs.acs.org>.

■ AUTHOR INFORMATION

Corresponding Author

*E-mail: doctorovich@qi.fcen.uba.ar.

Notes

The authors declare no competing financial interest.

■ ACKNOWLEDGMENTS

This work was financially supported by the University of Buenos Aires (UBACYT X065), ANPCyT (PICT 2010-2497), PME 01113, and CONICET. D.M. is the holder of the Israel Matz Professorial Chair of Organic Chemistry. The OTTLE cell was kindly provided by Prof. Dr. Wolfgang Kaim. We thank Prof. Dr. Carlos Brondino for supporting EPR measurements.

■ REFERENCES

- (1) (a) Goodrich, L. E.; Paulat, F.; Praneeth, V. K. K.; Lehnert, N. *Inorg. Chem.* **2010**, *49*, 6293–6316. (b) Roncaroli, F.; Videla, M.; Slep, L. D.; Olabe, J. A. *Coord. Chem. Rev.* **2007**, *251*, 1903–1930. (c) Feltham, R. D.; Enemark, J. H. *Top. Stereochem.* **1981**, *12*, 155–215. (d) Enemark, J. H.; Feltham, R. D. *Coord. Chem. Rev.* **1974**, *13*, 339–406.
- (2) Reviews: (a) Gunanathan, C.; Milstein, D. *Acc. Chem. Res.* **2011**, *44*, 588–602. (b) Pugh, D.; Danopoulos, A. A. *Coord. Chem. Rev.* **2007**, *251*, 610–641. (c) Szabó, K. J. *Synlett* **2006**, *6*, 811–824. (d) Rybtchinski, B.; Milstein, D. *ACS Symp. Ser.* **2004**, *885*, 70–85. (e) van der Boom, M. E.; Milstein, D. *Chem. Rev.* **2003**, *103*, 1759–1792. (f) Singleton, J. T. *Tetrahedron* **2003**, *59*, 1837–1857. (g) Milstein, D. *Pure Appl. Chem.* **2003**, *75*, 445–460. (h) Albrecht, M.; van Koten, G. *Angew. Chem., Int. Ed.* **2001**, *40*, 3750–3781. (i) Vignalok, A.; Milstein, D. *Acc. Chem. Res.* **2001**, *34*, 798–807. (j) Jensen, C. M. *Chem. Commun.* **1999**, 2443–2449. (k) Rybtchinski, B.; Milstein, D. *Angew. Chem., Int. Ed.* **1999**, *38*, 870–883.
- (3) Fe^{II} : (a) García Serres, R.; Grapperhaus, C. A.; Bothe, E.; Bill, E.; Weyhermüller, T.; Neese, F.; Wieghardt, K. *J. Am. Chem. Soc.* **2004**, *126*, 5138–5153. (b) Mu, X. H.; Kadish, K. M. *Inorg. Chem.* **1988**, *27*, 4720–4725. Ru^{II} : (c) Singh, P.; Das, A. K.; Sarkar, B.; Niemeyer, M.; Roncaroli, F.; Olabe, J. A.; Fiedler, J.; Zális, S.; Kaim, W. *Inorg. Chem.* **2008**, *47*, 7106–7113. (d) Singh, P.; Fiedler, J.; Zális, S.; Duboc, C.; Niemeyer, M.; Lissner, F.; Schleid, T.; Kaim, W. *Inorg. Chem.* **2007**, *46*, 9254–9261. (e) Videla, M.; Jacinto, J. S.; Baggio, R.; Garland, M. T.; Singh, P.; Kaim, W.; Slep, L. D.; Olabe, J. A. *Inorg. Chem.* **2006**, *45*, 8608–8617. (f) Sarkar, S.; Sarkar, B.; Chanda, N.; Kar, S.; Mobin, S. M.; Fiedler, J.; Kaim, W.; Lahiri, G. K. *Inorg. Chem.* **2005**, *44*, 6092–6099. (g) Sellmann, D.; Gottschalk-Gaudig, T.; Haussinger, D.; Heinemann, F. W.; Hess, B. A. *Chem.—Eur. J.* **2001**, *7*, 2099–2103. Os^{II} : (h) Singh, P.; Sarkar, B.; Sieger, M.; Niemeyer, M.; Fiedler, J.; Zális, S.; Kaim, W. *Inorg. Chem.* **2006**, *45*, 4602–4609. Ir^{III} : (i) Sieger, M.; Sarkar, B.; Zális, S.; Fiedler, J.; Escola, N.; Doctorovich, F.; Olabe, J. A.; Kaim, W. *Dalton Trans.* **2004**, 1797–1800.
- (4) (a) Cheng, P. T.; Nyburg, S. C. *Inorg. Chem.* **1975**, *14*, 327–329. (b) Einstein, F. W. B.; Sutton, D.; Vogel, P. L. *Inorg. Nucl. Chem. Lett.* **1976**, *12*, 671–675.
- (5) Gaviglio, C.; Ben-David, Y.; Shimon, L. J. W.; Doctorovich, F.; Milstein, D. *Organometallics* **2009**, *28*, 1917–1926.
- (6) (a) Halpern, J.; Maher, J. P. *J. Am. Chem. Soc.* **1965**, *87*, 5361–5366. (b) Chock, P. B.; Halpern, J. *J. Am. Chem. Soc.* **1969**, *91*, 582–588. (c) Kwiatek, J.; Seyler, J. K. *J. Organomet. Chem.* **1965**, *3*, 421–432. (d) Halpern, J.; Pribanic, M. *Inorg. Chem.* **1970**, *9*, 2616–2618. (e) Adamson, A. W. *J. Am. Chem. Soc.* **1956**, *78*, 4260–4261. (f) Vlcek, A. A.; Basolo, F. *Inorg. Chem.* **1966**, *5*, 156–158.
- (7) (a) Wrighton, M. S.; Ginley, D. S. *J. Am. Chem. Soc.* **1975**, *97*, 2065–2072. (b) Wrighton, M. S.; Ginley, D. S. *J. Am. Chem. Soc.* **1975**, *97*, 4246–4251. (c) Kuksis, I.; Kovács, I.; Baird, M. C. *Organometallics* **1996**, *15*, 4991–5002.
- (8) (a) Puschmann, F. F.; Grützmacher, H.; de Bruin, B. *J. Am. Chem. Soc.* **2010**, *132*, 73–75. (b) Sofranko, J. A.; Eisenberg, R.; Kampmeier, J. A. *J. Am. Chem. Soc.* **1980**, *102*, 1163–1165. (c) Pilloni, G.; Zotti, G.; Zecchini, S. *J. Organomet. Chem.* **1986**, *317*, 357–362. (d) Mueller, K. T.; Kunin, A. J.; Greiner, S.; Henderson, T.; Kreilick, R. W.; Eisenberg, R. *J. Am. Chem. Soc.* **1987**, *109*, 6313–6318. (e) Kunin, A. J.; Nanni, E. J.; Eisenberg, R. *Inorg. Chem.* **1985**, *24*, 1852–1856.
- (9) Frech, C. M.; Ben-David, Y.; Weiner, L.; Milstein, D. *J. Am. Chem. Soc.* **2006**, *128*, 7128–7129.
- (10) (a) Zhu, D.; Budzelaar, P. H. M. *Organometallics* **2010**, *29*, 5759–5761. (b) Zhu, D.; Korobkov, I.; Budzelaar, P. H. M. *Organometallics* **2012**, *31*, 3958–3971.
- (11) Di Vaira, M.; Ghilardi, C. A.; Sacconi, L. *Inorg. Chem.* **1976**, *15*, 1555–1561.
- (12) Thyagarajan, S.; Incarvito, C. D.; Rheingold, A. L.; Theopold, K. H. *Inorg. Chim. Acta* **2003**, *345*, 333–339.
- (13) Tomson, N. C.; Crimmin, M. R.; Petrenko, T.; Rosebrugh, L. E.; Sproules, S.; Boyd, W. C.; Bergman, R. G.; DeBeer, S.; Toste, F. D.; Wieghardt, K. *J. Am. Chem. Soc.* **2011**, *133*, 18785–18801.
- (14) Verat, A. Y.; Pink, M.; Fan, H.; Fullmer, B. C.; Telsler, J.; Caulton, K. G. *Eur. J. Inorg. Chem.* **2008**, *30*, 4704–4709.
- (15) Frech, C. M.; Shimon, L. J. W.; Milstein, D. *Helv. Chim. Acta* **2006**, *89*, 1730–1739.
- (16) Connelly, N. G.; Geiger, W. E. *Chem. Rev.* **1996**, *96*, 877–910.
- (17) Bultitude, J.; Larkworthy, L. F.; Mason, J.; Povey, D. C.; Sandell, B. *Inorg. Chem.* **1984**, *23*, 3629–3633.
- (18) Vignalok, A.; Milstein, D. *Organometallics* **2000**, *19*, 2061–2064.
- (19) Richter-Addo, G. B.; Wheeler, R. A.; Hixson, C. A.; Chen, L.; Khan, M. A.; Ellison, M. K.; Schulz, C. E.; Scheidt, R. *J. Am. Chem. Soc.* **2001**, *123*, 6314–6326.
- (20) (a) Wei, Z.; Ryan, M. D. *Inorg. Chem.* **2010**, *49*, 6948–6954. (b) Pellegrino, J.; Hübner, R.; Doctorovich, F.; Kaim, W. *Chem.—Eur. J.* **2011**, *17*, 7868–7874.
- (21) Curran, D. P.; Keller, A. I. *J. Am. Chem. Soc.* **2006**, *128*, 13706–13707.
- (22) Frisch, M. J.; Trucks, G. W.; Schlegel, H. B.; Scuseria, G. E.; Robb, M. A.; Cheeseman, J. R.; Montgomery, J. A., Jr.; Vreven, T.; Kudin, K. N.; Burant, J. C.; Millam, J. M.; Iyengar, S. S.; Tomasi, J.; Barone, V.; Mennucci, B.; Cossi, M.; Scalmani, G.; Rega, N.; Petersson, G. A.; Nakatsuji, H.; Hada, M.; Ehara, M.; Toyota, K.; Fukuda, R.; Hasegawa, J.; Ishida, M.; Nakajima, T.; Honda, Y.; Kitao, O.; Nakai, H.; Klene, M.; Li, X.; Knox, J. E.; Hratchian, H. P.; Cross, J. B.; Bakken, V.; Adamo, C.; Jaramillo, J.; Gomperts, R.; Stratmann, R. E.; Yazyev, O.; Austin, A. J.; Cammi, R.; Pomelli, C.; Ochterski, J. W.; Ayala, P. Y.; Morokuma, K.; Voth, G. A.; Salvador, P.; Dannenberg, J. J.; Zakrzewski, V. G.; Dapprich, S.; Daniels, A. D.; Strain, M. C.; Farkas, O.; Malick, D. K.; Rabuck, A. D.; Raghavachari, K.; Foresman,

J. B.; Ortiz, J. V.; Cui, Q.; Baboul, A. G.; Clifford, S.; Cioslowski, J.; Stefanov, B. B.; Liu, G.; Liashenko, A.; Piskorz, P.; Komaromi, I.; Martin, R. L.; Fox, D. J.; Keith, T.; Al-Laham, M. A.; Peng, C. Y.; Nanayakkara, A.; Challacombe, M.; Gill, P. M. W.; Johnson, B.; Chen, W.; Wong, M. W.; Gonzalez, C.; Pople, J. A. *Gaussian 03*, Revision C.02; Gaussian, Inc.: Wallingford, CT, 2004.

(23) Connelly, N. G.; Draggett, P. T.; Green, M.; Kuc, T. A. *J. Chem. Soc., Dalton Trans.* **1977**, 70–73.